Bogajo, I.R., Tangpronprasert, P., Virulsri, C. *et al.* A novel indirect cryogenic cooling system for improving surface finish and reducing cutting forces when turning ASTM F-1537 cobalt-chromium alloys. *Int J Adv Manuf Technol* **111**, 1971–1989 (2020). https://doi.org/10.1007/s00170-020-06193-x

TITLE:

A novel indirect cryogenic cooling system for improving surface finish and reducing cutting forces when turning ASTM F-1537 cobalt chromium alloys

AUTHORS

*Iñigo Rodriguez Bogajo; **Pairat Tangpronprasert; **Chanyapan Virulsri; **Saran Keeratihattayakorn; *Pedro José Arrazola

*Faculty of Engineering, Mondragon University, Loramendi 4, Arrasate 20500, Spain

**Center Of Excellence for Prosthetic And Orthopedic Implant, Department of Mechanical Engineering, Faculty Of Engineering, Chulalongkorn University, Phayathai Road, Pathumwan, Bangkok 10330, Thailand

CONTACT

Iñigo Rodriguez Bogajo; email: inigo.rodriguez@alumni.mondragon.edu

KEYWORDS

Indirect cryogenic cooling; Liquid nitrogen; cobalt based alloys; cryogenic turning

ABSTRACT

This paper presents a novel indirect cryogenic cooling system, employing liquid nitrogen (LN_2) as a coolant for machining the difficult-to-cut ASTM F-1537 cobalt chromium (CoCr) alloy. The prototype differs from the already existing indirect cooling systems by using a modified cutting insert that allows a larger volume of cryogenic fluid to flow under the cutting zone. For designing the prototype analytical and finite element thermal calculations were performed, this enabled to optimize the heat evacuation of the tool from the rake face without altering the stress distribution on the insert when cutting material. Turning experiments on ASTM F-1537 CoCr alloys were performed under different cutting conditions and employing indirect cryogenic cooling and dry machining, to test the performance of the developed system. The results showed that the new system improved surface roughness by 12%, and cutting forces were also reduced by 12%, when compared to existing indirect cryogenic cooling technique.

LIST OF SYMBOLS

TOOL GEOMETRICAL PARAMETERS

$Ø_{eff}$	Effective diameter of the tool (m)
t	Top wall thickness of the insert (m)
w	Side wall thickness of the insert (m)
L_{INS}	Side length of the cutting insert (m)
t_{insert}	Thickness of the cutting insert (m)

CUTTING PARAMETERS

F_t	Frictional force (N)
V_s	Sliding velocity (m/s)
V_c	Cutting speed (m/min)
f	Feed (mm/rev)
a_p	Depth of cut (mm)

F_c	Cutting force (N)
F_f	Feed force (N)
F_p	Passive force (N)

THERMAL QUANTITIES

$\dot{Q}$	Heat transfer rate (W)
$\dot{q}_t$	Heat transfer rate from chip to the tool (W)
ξ	Fraction of the energy generated at the tool-chip interface that remains with the chip material
α	Thermal diffusivity (m^2/s)
c_p	Specific heat (J/kg K)
T_{CHIP}	Temperature of the chip (K)
T_{RAKE}	Temperature at the rake face of the tool (K)
T_{CRYO}	Temperature of the cryogenic media at the back of the tool (K)
R_{SPR}	Spreading thermal resistance on the rake face of the tool
R_{COND}	Conductive thermal resistance of the tool insert
R_{BOIL}	Convective thermal resistance of the nitrogen in gas phase
R_{CONV}	Convective thermal resistance of the nitrogen in liquid phase
k	Thermal conductivity (W/(m K))
k_t	Thermal conductivity of the tool (W/(m K))
h	Convective coefficient ($W/(m^2 K)$)
h_{N2}	Convective coefficient of nitrogen in gas phase ($W/(m^2 K)$)
h_{LN2}	Convective coefficient of nitrogen in liquid phase ($W/(m^2 K)$)
A_{cav}	Surface available for heat exchange in the cavity generated in the tool insert (m^2)
L_c	Characteristic length of the of the body to which the heat is being transferred to
Nu	Nusselt number

MECHANICAL QUANTITIES

μ	Friction coefficient

1 INTRODUCTION

Cobalt based alloys are used in aeronautics, gas turbines and biomedical applications owing to their high temperature strength and good corrosion resistance [1]. The ASTM F-1537 CoCr alloy is of particular interest for manufacturing orthopaedic implants since it forms a hard-passive oxide layer on the surface, which makes it bio-compatible [2]. Cobalt based super alloys are usually alloyed with Molybdenum (Mo) or Tungsten (W) to increase strength, an important property for prosthetics. In addition, increasing the chromium content improves corrosion resistance and increases hardness as a result of carbide formation.

However, the aforementioned properties that make ASTM F-1537 CoCr alloys ideal for orthopaedics, together with their poor thermal conductivity, have earned them a reputation as difficult-to-cut materials, as is the case of other alloys employed for medical purposes like Ti-6Al-4V [2]. CoCr alloys are challenging materials to machine due to their strengthening mechanisms which consist of the formation of carbides, solid solution strengthening and formation of intermetallic compounds. These mechanisms increase the specific energy required to cut the material, which added to the low thermal conductivity (about 10 W/m K), cause a considerable increase in temperature in the cutting tool [3].

Rapid tool wear and poor surface integrity of the machined parts are the main drawbacks of these difficult-to-cut alloys. The former is mainly caused by the work hardening and attrition properties of the material, while the latter is a consequence of heat generation and plastic deformation [4].

Dimensional accuracy and controlled surface roughness are important aspects in the machining of prosthetics, since they can affect the success of subsequent finishing operations such as drag or vibratory finishing [6]. These final operations give a controlled texture to the surface of the component, which will promote the response of the tissues and the integration of the implant in the patient [5], however they don't allow the correction of dimensional errors. Thus, dimensional accuracy in processes prior to finishing should be considered carefully, and as a result, cutting forces need to be restricted.

Cutting fluids, and especially high-pressure coolant supplies [6] have been seen to promote a significant improvement in tool life, surface finish and surface integrity due to their capability of extracting heat and lubricating the cutting zone [7], [8]. As the most commonly used metalworking fluids (MWFs) are oil based however, they can create several environmental and health problems, such as water pollution and soil contamination at disposal, in addition to generation of fumes, which can be hazardous for workers [9].

In the case of prosthetics, contaminating the implant with oil-based fluids can create allergic and inflammatory responses in the patient. Amongst the most notorious cases of MWF contamination in prosthetics, is that of the hip replacements of Sulzer Inter OP™ [10]. Contaminants were found in the recalled lots of the implants manufactured by this company, including machine oil residues. A study examining the tissue response to machine oil concluded that the presence of oils on the implant surface inhibited fixation of the prosthetic and osseointegration [11]. Thus, eliminating the usage of oils for machining orthopaedic components is a significant issue, since cleaning such parts is difficult and expensive [12]. Similar problems with MWFs were found in other case studies where implants contaminated with oil-based residue and mixed with debris and other substances at the time of manufacturing caused tissue inflammation in several patients [13].

To address these health and environmental issues, and to improve machinability of difficult-to-cut materials, extensive research is being conducted for developing new machines and methods that are based on the use of a

small amount of cooling and lubrication, the study of feasibility of dry machining of the use of cryogenic fluids as coolant [14]. A comparative study between different alternative cooling techniques was carried out by Benedicto et al. [15]. In their study, not only the performance and the environmental impact of the different cooling methods was analysed, but also the cost of further cleaning machined parts or the easiness of recycling the produced chips. As they stated Minimum Quantity Lubrication (MQL) is one of the most economically viable alternatives which provides lubrication of the cutting zone without using excess of MWFs. On the other hand, cryogenic cooling is a technique that can lengthen the tool life with very low environmental impact, and without needing to clean oils form the machined part. Even though the initial cost is higher.

The extensive literature review published by Binayak et al. [16] reducing the use of oil by Minimum Quantity Lubrication (MQL) technique, and applying the lubricant at the correct nozzle angle and distances, can improve the surface integrity of the machined parts compared to when using flood cooling. Also, they provide the opportunity to combine them with hybrid nanoparticles to improve the lubricity of the fluid, but on the downside the toxicity of such nanoparticles and the actual environmental impact of MQL oils using Life Cycle Assessment tools in still unknown, according to Binayak et al. [16]. In addition to this the use of oils, even if they are supplied in small quantities, is not recommended for machining prosthetics.

On the other hand, cryogenic cooling could be an environmentally and health friendly solution to machine prosthetics. This technology was first introduced by Hong [17]. In this study a specially designed micro-nozzle was used to deliver liquid nitrogen (LN_2) to the cutting zone, thus achieving an effective method of cooling the tool using a small flow of LN_2 (Fig. 1, a). Several research works have followed this same technique when machining different difficult-to-cut alloys [18]–[21]. Mozzammel et al. [22] carried out a detailed analysis of process parameters and LCA of turning Ti-6Al-4V alloy with assistance of LN_2. Such research work shows that using LN_2 as a coolant is more environmentally friendly than machining in dry conditions, due to the enhancement in machinability brought up by the cryogenic cooling. According to Mozammel et al. [22] the specific cutting force required to turn Ti-6Al-4V is reduced when cooling the cutting zone with LN_2 supplied by micro-nozzles. This in turn reduced the energy consumption of the machine in comparison to dry cutting. Such improvement in machinability can be further increased if two nozzles are used impinging on rake and flank faces.

Nevertheless, the feasibility of this cooling technique is still not fully understood, since as opposed to conventional cooling, cryogenic jet cooling is highly sensitive to the position of the nozzles in respect to the cutting tool and workpiece [23]–[25]. In some cases, the LN_2 can overcool the workpiece or fail to impinge on the tool-chip interface correctly, bringing about adverse results in tool life and surface integrity [26], [27].

The literature has shown that to achieve a cooling system that improves machinability of the material it is necessary to maintain the workpiece at a temperature at which the material is ductile, while keeping the cutting tool as cool as possible [28]. For this reason, indirect cryogenic cooling (also known as cryogenic tool back cooling) was investigated by Hong and Ding [29]. Their method consists of cooling the main heat source (the cutting point), through heat conduction from a LN_2 chamber located below the tool insert [30]. In this way, the carbide insert is maintained at low temperatures without making significant changes to the properties of the material.

Current investigations into indirect cryogenic cooling focus on modifying the shim or the tool holder of the cutting tool to allow LN_2 to flow through the tool and expand near the main heat source (Fig. 1, b) [17], [31]–[33].These studies report that although surface roughness is improved, heat due to friction is still considerable, as the rake and flank

faces of the tool are not lubricated and problems due to Built-up-Edge (BUE) appear. These authors recognise that the efficiency of indirect cryogenic cooling is strongly dependant on the heat exchange surface area available for the LN_2 to evacuate the heat. The study by Sarikaya and Güllü [34] showed that indirect cryogenic cooling increased tool life in comparison to dry cutting for different cutting speeds when turning Haynes 25 cocr alloy. As they reported tool life was increased by 60% when cooling the cutting zone indirectly with cryogenic media, but adhesive and diffusive tool wear mechanisms were present both in dry cutting and cryogenically aided cutting.

Another important design aspect which influences the feasibility of indirect cooling systems is heat transfer through the cutting insert. As Minton et al. stated [35], indirect cooling of cutting tools requires the high heat generated on the rake face to be extracted via conduction through an insert, which is limited in its thermal conductivity. It is thus necessary to situate the cooling effect as close to the cutting edge as possible, to negate the low thermal conductivity of the cutting insert, whilst maintaining the mechanical strength of the insert.

To improve surface roughness and reduce cutting forces when dry machining ASTM F-1537 CoCr alloys, a new indirect cryogenic cooling system is proposed in this paper. This novel design has a modified cutting insert which allows the LN_2 to flow nearer to the rake face thereby increasing the surface available for heat exchange (Fig. 1, c). These modifications are proposed with the objective of enhancing the heat dissipation capability of the indirect cooling system, and improving the cutting performance of the tool.

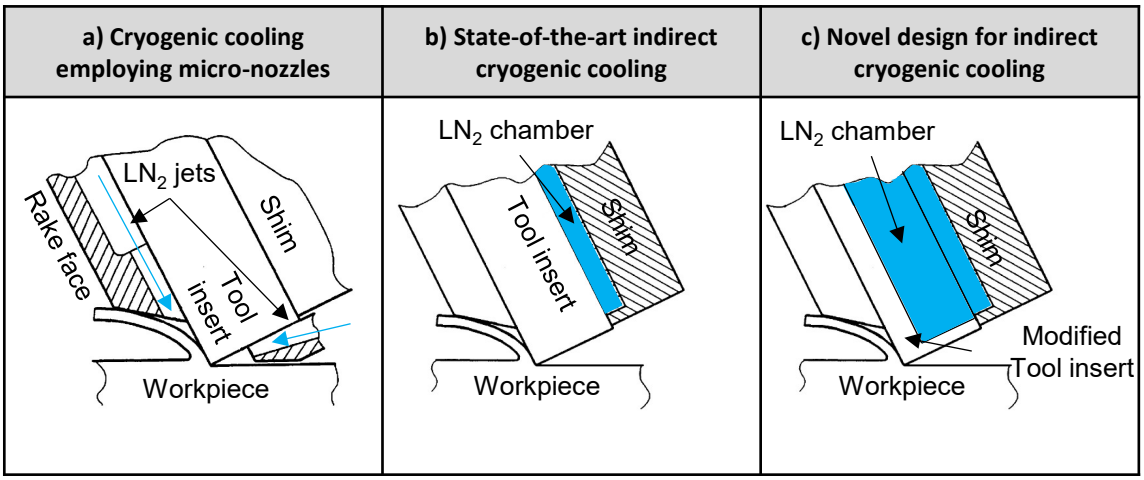

Fig. 1 Supply methods of cryogenic medium: a) and b) currently employed cryogenic cooling methods [30], adapted. c) novel design for indirect cryogenic cooling proposed in this study

In this paper, a design based on analytical calculations and FEM simulations for new indirect cryogenic cooling system is introduced. Then, the experimental validation of the results is shown. Finally, the main conclusions are presented, comparing state-of-the-art indirect cryogenic systems and the novel design presented in this study.

2 TOOL INSERT DESIGN FOR INDIRECT COOLING

Two different thermal models were used in order to design the indirect cryogenic cooling system. The analytical model was carried out in order to have an approximate idea of how the heat evacuation capacity of the insert varied when different cavity geometries were machined, and when different heat fluxes were transferred to the tool. Once an optimized modified tool geometry was defined a thermomechanical analysis for stress and temperatures were carried out in order to validate the prototype, using the FEM model. This detailed analysis was more easily carried out with the numerical model than with analytical model.

2.1 Analytical model

To optimize the dimensions of the cavity machined at the insert, an analytical heat transfer model proposed by Rozzi et al. [36] was followed. In that model a value for the heat transfer rate (q_t) from the chip to the tool is estimated. Then, the tool is modelled as a set of thermal resistances so as to calculate the heat evacuation capacity of the LN_2 in the indirect cryogenic cooling system.

In metal cutting there are different heat sources responsible for the rise in temperature in the tool-workpiece couple. Two main origins can be identified: contact with friction at the tool workpiece interface, and plastic deformation in the chip [37]. As Fig. 2 depicts, the former source of heat occurs in the secondary shear zone, and is mainly dependant on the friction coefficient between the chip and the tool material. The latter source of heat is generated in the primary shear zone due to plastic work and it is transferred to the tool indirectly due to thermal conduction.

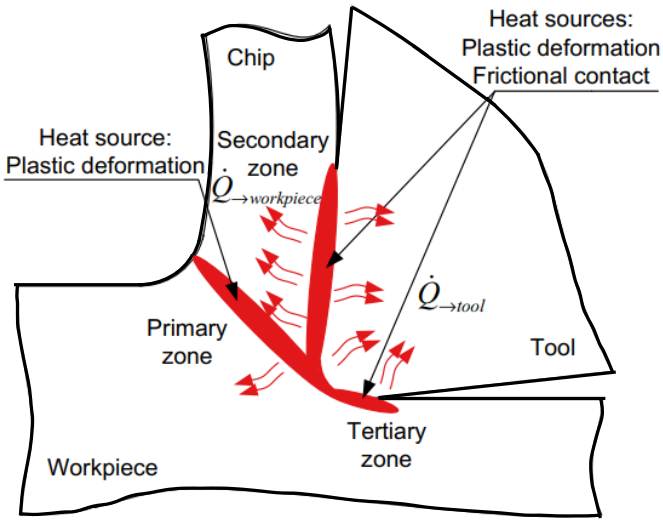

Fig. 2 Main heat sources during chip formation in machining [37]

Komanduri et al. [38] considered the effect of the primary shear zone on the final temperature rise within the tool by introducing an induced stationary heat source, caused by the primary heat source. They observed that the effect of the tool-chip interface frictional heat source on the temperature rise at the interface was predominant, as the rise in temperature bought about by the deformation in the primary shear zone was around 200 K. In the case of machining steel under conventional cutting conditions, they also found that the maximum temperature rise at the tool-chip interface (secondary shear zone) was located away from the tool tip.

For this reason, in the present paper the calculus for the heat transfer rate principally considers the frictional forces on the rake face of the insert, as shown in Expression 1. Nonetheless, 3 different tool-chip interface temperatures are taken into account in the calculus. To this end a first approach was carried out to evaluate the effect changing the temperature of the tool-chip interface has on the heat transferred to the tool. Hence, the effect of considering the temperature rise generated in the primary shear zone as a stationary heat source could be determined.

$$\dot{q}_t = (1 - \xi)\, F_t\, V_s \qquad (1)$$

Expression 1 calculates the heat transferred to the tool due to frictional forces. ξ is the fraction of energy generated at the tool-chip interface that remains with the chip material, and F_t is the frictional force in the tool in orthogonal machining. V_s is the sliding velocity between the workpiece and tool considered for the calculation, which affects the friction coefficient between tool and workpiece. The heat transfer rate is dependant of tool geometry, mechanical properties of the material and relative sliding between tool and chip. As regards the geometry of the tool, an orthogonal model with 0° rake angle was considered for simplicity of calculus.

There are few studies in which cutting temperature has been measured when dry turning Cobalt based alloys, but as Baron et al. stated [2] the specific energy necessary to turn the ASTM F-1537 CoCr alloy is equal or greater than that of Ti-6Al-4V. For this reason, the cutting temperatures of around 1000K when dry turning Ti-6Al-4V alloys at 50 m/min and 0.1 mm/rev measured by Kitagawa et al. were considered as a reference [39]. Thus, considering that the mechanical properties of ASTM F-1537 CoCr alloys are slightly more demanding than those of Ti-6Al-4V alloys, and that the cutting conditions expected for the experimental plan were heavier than those employed by Kitagawa et al., temperatures ranging from 1000K to 1200 K were assumed in this study.

To calculate the fraction of energy generated that remains with the chip material (ξ), it is necessary to know the thermal properties of the material at the shear plane [36]. In the present study it was assumed that the temperature of the material at the shear plane is at a temperature of 850 K. This assumption was based on the thermal gradients recorded by other authors in dry machining hard-to-cut Grade 2 CP Titanium alloys [35].

As the thermal and mechanical properties of the ASTM F-1537 CoCr alloy are susceptible to temperature, different values for thermal diffusivity, specific heat and shear strength had to be measured, depending on the temperature of the chip in consideration. It was also assumed that the area of the cutting insert in contact with the workpiece would be the same temperature as the chip. Accordingly, different thermal conductivity values for the carbide insert were assumed. The temperature dependant mechanical and thermal properties of the ASTM F-1537 CoCr alloy shown in Table 1, were obtained from the datasheet of the material [40]. In addition, the thermal conductivity of the carbide insert was measured by Nordgrena et al. [41].

Table 1: Temperature dependant mechanical and thermal properties of tool and workpiece materials

	Chip			**Shear plane**
Temperature (K)	1200	1100	1000	850
Thermal diffusivity (m^2/sec)	4.92 E-06	4.86 E-06	4.65 E-06	4.2 E-06
Specific heat (J/kg K)	610	601	591	545
Shear strength of the ASTM F-1537 CoCr workpiece (N/m^2)	4.07 E07	4.93 E07	5.10 E07	X
Thermal conductivity of the P10 grade carbide tool (W/(m·K))	66.3	64.4	63.1	X

To calculate the evolution of the heat transfer due to friction at different cutting conditions, the friction coefficients for different sliding speeds were taken from Aherwar et al. [42]. In that study the friction coefficients at different sliding speeds between hardened steel (70 HRC) and the Co30Cr4Mo biomedical alloy were obtained experimentally. The contact pressure employed in the experiments was 15 N and the alloy had 0% Nickel content. As opposed to research carried out with other hard-to-cut materials [17], in the study carried out by Aherwar et al. [42] the friction coefficient increased at the highest sliding speed. This increase in friction coefficient at high cutting speeds was also observed by Bhansali [43] when analysing adhesive wear of cobalt chromium alloys. They stated that this increase in adhesive wear was related to the formation of NiP-Cr_2O_3 spinel oxides when transitioning from mild to high loads. The friction values as a function of the sliding velocity are set out in Table 2.

It is known that chip thickness is greater than the uncut chip thickness due to the plastic strain and high temperatures occurring in the cutting zone [44]. As the chip swells, the chip velocity becomes lower than the cutting speed, and thus the mass flow remains constant. In the case of medical grade cobalt chromium alloys, for cutting speeds between 30 m/min and 90 m/min and feed values between 0.01 mm/rev and 0.09 mm/rev ,shear localized (saw tooth) chips have been obtained by some authors [45], [46]. When saw tooth chips are obtained the chip thickness is hard to evaluate. For this reason, in this calculus the chip sliding speed was assumed to be roughly the same as the cutting speed. Cutting speeds ranging between 15 m/min (0.25 m/s) and 80 m/min (1.3 m/s) were assumed in the analytical model.

Table 2: Friction coefficient values between carbide and the ASTM F-1537 CoCr alloy for different sliding speeds [42]

Sliding speed, V_s (m/s)	0.26	0.52	0.78	1.04	1.3
Friction coefficient, μ	0.42	0.45	0.42	0.46	0.66

Following expression 1, the heat transferred to the tool (q_t) was calculated for different sliding speeds and chip temperatures. Even though 3 different chip temperature values were taken into account in the calculus, it was assumed that this temperature would be constant for different sliding speeds.

The heat transfer rate (q_t) calculated with expression 1 was assumed to be the amount of energy the indirect cryogenic cooling system needs to dissipate to maintain the LN_2 inside the machined cavity at a saturated boiling state. To complete the thermal model, the materials and cooling fluids comprising the indirect cryogenic cooling were considered as thermal resistances with different conductive and convective coefficients.

As sliding speed and frictional forces increase, the amount of heat required for the indirect cryogenic cooling system to dissipate also increases. Therefore, a greater amount of heat needs to be dissipated, requiring a larger LN_2 chamber and a smaller insert top wall thickness (t). As the top wall thickness of the insert decreases a greater surface becomes available for heat exchange in the LN_2 chamber. In addition, the conductive resistance generated by the carbide insert (R_{COND}) will be reduced.

The temperature on the rake face of the tool (T_{RAKE}) was assumed to be the same as the chip temperature (T_{CHIP}) considered in each case, thus ranging from 1000 K to 1200 K. The temperature inside the LN_2 chamber (T_{CRYO}) was assumed to be 90 K, which corresponds to that of saturated boiling LN_2 at ambient pressure (1 atm). Considering the thermal model as a set of resistances (see expression 2), and knowing the temperatures at each end of the set

of resistances, an optimal value of insert top wall thickness (t) can be calculated for each value of heat transfer rate (q_t). As previously mentioned, the heat transfer rate changes for different sliding speeds (V_s), therefore an optimal insert top wall thickness was obtained for several sliding speeds. This was achieved, by solving the parameter "t" from Expression 3.

$$R_{SPR} + R_{COND} + R_{BOIL} + R_{CONV} = \frac{T_{RAKE} - T_{CRYO}}{q_t} \quad (2)$$

$$\frac{1}{2\,\emptyset_{eff}\,k_t} + \frac{t}{k_t\,A_{cav}} + \frac{1}{h_{N2}\,A_{cav}} + \frac{1}{h_{LN2}\,A_{cav}} = \frac{T_{RAKE} - T_{CRYO}}{q_t} \quad (3)$$

The surface area available for heat exchange (A_{cav}) is a relevant parameter which determines the effectiveness of the indirect cryogenic cooling system [31]–[33]. Accordingly, in addition to the insert top wall thickness (t), the insert side wall thickness (w) is also an important geometrical parameter, as Expression 4 shows. For this first approach in which the relevance of varying the assumed temperature of the chip (T_{CHIP}) is analysed, a constant side wall thickness (w) value of 1.5 mm was assumed. Estimating that the depth of cut in the experimental tests would be 1 mm, it was assumed that a side wall thickness (w) of 1.5 mm would provide enough strength to the modified insert. This is because the material being cut is supported by the whole thickness of the insert. Following the calculus performed by Rozzi et al. [36] a spreading resistance (R_{SPR}) was taken into account in the calculus as the tool-chip interface area is small compared with the size of the turning insert. The thickness of the cutting insert (t_{insert}) was 4.76 mm.

$$A_{cav} = (L_{INS} - 2\,w)^2 + 4\,(L_{INS} - 2\,w\,)\,(t_{insert} - t) \quad (4)$$

In indirect cryogenic cooling systems, the cryogenic fluid flows in and out of the cavity placed beneath the cutting insert to extract heat form the cutting zone through conduction. In this study the formation of a nitrogen gas film of the surface of the insert was also taken into consideration (R_{BOIL}), as the nitrogen inside the chamber was assumed to be at saturated boiling state.

To calculate the thermal resistances introduced by the LN_2 (R_{CONV}) and the boiling nitrogen gas film (R_{BOIL}), the convective heat transfer coefficients for LN_2 (h_{LN2}) and gaseous nitrogen (h_{N2}) were consecutively calculated, according to a fixed flow rate. A flow rate of 0.05 m^3/s was assumed considering that most of LN_2 tanks operate at a pressure of 1.5 bar and that the nitrogen gas would be released to atmospheric pressure (1 atm). A representation of the set of thermal resistances used to model the new modified indirect cryogenic cooling system is shown in Fig. 3.

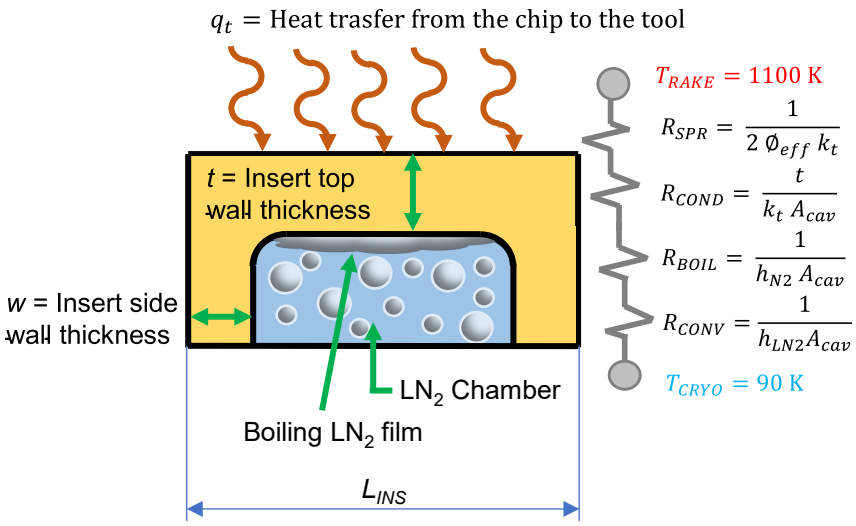

Fig. 3 Model of heat transfer employed in the tool insert.

Following the equation for the Nusselt number "*Nu*" [47], the convective coefficient (*h*) can be calculated for liquid flowing at a certain flow rate and state, as seen in Expression 5. The Nusselt number represents the enhancement of heat transfer through a fluid layer as a result of convection relative to conduction across the same fluid layer. The larger the Nusselt number, the more effective the convection. A Nusselt number of Nu = 1 for a fluid layer represents heat transfer across de layer by pure conduction, for example [47]. Therefore, a higher Nusselt number would increase the heat transfer coefficient "h" of the fluid.

The thermal conductivity "*k*" of the fluid and L_c the characteristic length of the body to which the heat is being transferred to. Thermal conductivity of liquid nitrogen at 90 K was considered to be k_{LN2} = 7.7 E-03 W/m K, whereas that of gaseous nitrogen at 313 K was k_{N2} = 9.5 E - 06 W/m K [48]. The Nusselt number "*Nu*" is determined by the state of the flow of the nitrogen and other dimensionless numbers, such as Reynolds number and Prandtl number [47]. Following Expression 5 a heat transfer coefficient of h_{LN2} = 250 W/m^2 K was obtained for the nitrogen in liquid state, and a convective heat transfer of h_{N2}=0.25 W/m^2 K was calculated for the gaseous nitrogen which forms a thin film of gas at the surface of the machined pocket in the insert.

$$h = \frac{Nu\,k}{L_c} \tag{5}$$

In Fig. 4 the variation of the heat transfer rate for 3 different chip temperature values (1000, 1100 and 1200 K) and sliding speeds can be observed. The insert top wall thickness (*t*) values required for a proper evacuation of that heat are also plotted for each case. It can be seen that the greatest variation of this geometrical parameter for different temperatures occurs at the highest sliding speeds, with a fluctuation of around 1 mm. Except for the highest sliding speed values for a chip temperature of 1000 K, all top wall insert (*t*) values are greater than 2 mm, which indicates that the indirect cryogenic cooling system is able to evacuate the heat properly without the presence of the machined pocket at low sliding speeds.

Lower chip temperatures generate the highest amount of heat transfer to the tool. This result is likely due to the model being heavily dependent on the shear strength of the material. The shear strength of the ASTM F-1537 CoCr alloy is significantly affected by the increase in temperature (Table 1). The reduction in shear strength at high chip temperatures generates lower frictional forces, which result in a lower heat transfer to the tool. It is true that at higher

temperatures the thermal diffusivity and heat capacity of the ASTM F-1537 CoCr alloy increase, which would result in improved heat carrying capacity for the chip. However, this change in thermal properties is outperformed by the decrease in shear strength the material experiences.

As the comparison in Fig. 4 shows, a change of 100 K does not greatly affect the amount of heat transferred to the tool. The heat transfer rate to the tool does not change more than 5 W with a change of 100 K in chip temperature, even at high cutting speeds. For this reason, the central value of the analysed range of chip temperatures (T_{CHIP} = 1100 K) was selected for the posterior calculations.

Once T_{CHIP} was defined another calculation was made to evaluate the effect of the thickness of the side wall of the insert's machined cavity (w). As previously mentioned, this geometrical parameter affects the available surface for heat transfer, so its optimization is equally as important as finding the appropriate insert top wall thickness (t).

Three different values of insert side wall thickness were taken: 0.5 mm, 1.5 mm, and 2.5 mm. For each a value for A_{cav} was calculated using Expression 4, and then the insert top wall thickness (t) was calculated from the set of thermal resistances employed in Expression 3.

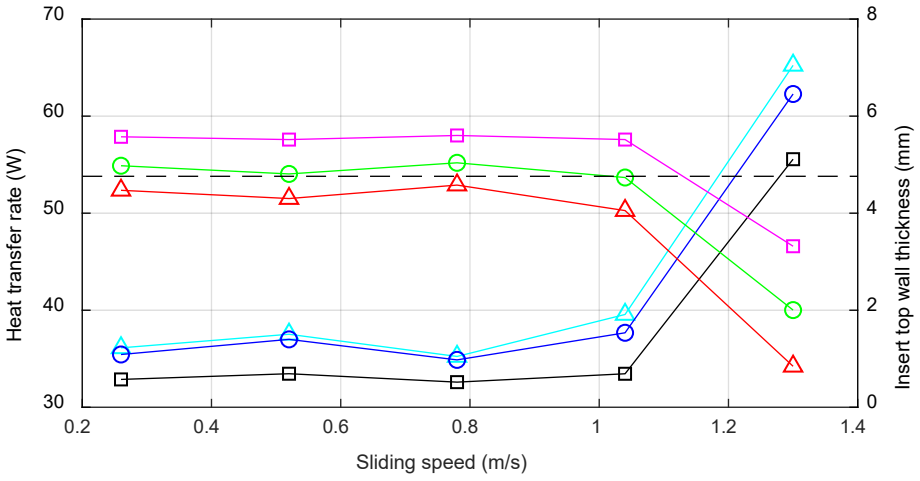

Fig. 4 Heat transferred to the tool and insert thickness required for evacuating transferred heat for different chip temperatures

The required top wall thickness (t) values for different side wall thickness (w) values are shown in Fig. 5. As was expected, when using a larger side wall thickness (w) the top wall thickness (t) required for evacuating the heat transferred to the tool (q_t) was smaller. This occurs because, as the side wall thickness (w) increases, the surface available for heat transfer (A_{cav}) is reduced. Therefore, a thinner top wall thickness is required to remove the heat.

A side wall thickness of 0.5 mm allows a thicker top wall thickness (t) while still evacuating the heat properly. Nevertheless, a side wall thickness smaller than the uncut chip thickness can compromise the performance of the cutting tool. This would cause the uncut material to apply pressure on part of the machined cavity instead of the whole thickness of the insert, shortening its life prematurely as the material being cut is not supported by the whole thickness of the insert. On the other hand, a side wall thickness of 2.5 mm would require an insert top wall thickness (t) of less than 1 mm at high sliding speeds.

In order to have a side wall with a thicker than the uncut chip thickness, while still maintaining a top wall thickness greater than 1 mm, a side wall thickness (w) of 1.5 mm was selected. This side wall thickness (w) was assumed to be thick enough to support uncut chip thickness values of around 1 mm, while still having an insert top wall thickness (t) of 2 mm at high sliding speeds, and enabling proper evacuation of heat transferred to the tool.

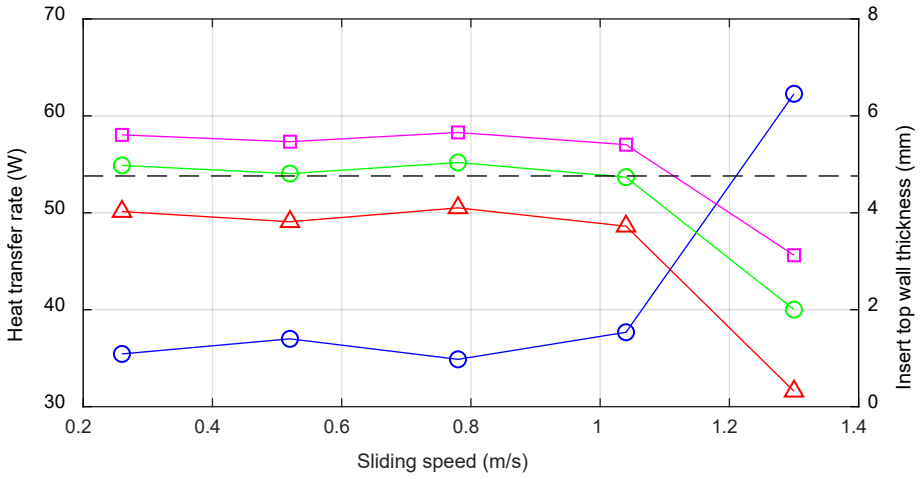

Fig. 5 Heat transferred to the tool at T_{CHIP} = 1100 K and insert thickness required for evacuating transferred heat for different values of insert side wall thickness (w)

2.2 FEM simulations

Following the results from the analytical calculus, a top wall thickness (t) of 2 mm and a side wall thickness (w) of 1.5 mm were taken as the geometrical parameters to define the cavity machined in the insert. The design of the prototype resulting from the analytical model was validated using a thermal calculation in an FEM model. In addition, a static analysis was performed to compare the stress distribution in the tool insert with and without the machined pocket, as seen in Fig. 6. SolidWorks simulation software was used for simulating both analyses.

Regarding the stress analysis of the designed prototype two main aspects need to be in consideration. First the potential effect that the modification may have brought up in the stress distribution of the cutting tool when performing machining operations. When carrying out cuts under dry conditions with the modified tool, the machined pocket might weaken the tool and cause tool failure due to an unfavourable stress distribution compared to non-modified inserts.

On the other hand, the abrupt change in temperatures from the cold sink at the cryogenic reservoir to the heat in the cutting zone may cause thermal cracking or degradation of fracture toughness properties of the tool material [49].

As the objective of the numerical stress calculation is to validate that the geometry of the modified inserts will stand dry cutting conditions, the Von Mises stress distributions was evaluated after the FEM simulations. It was decided that the potential problems regarding the cracking of the tool or problems due to thermal shock would be observed during the experimental trials.

For the thermal analysis, different convective coefficients were applied to the surfaces of the insert, depending on whether they were in contact with LN_2 or air from the surrounding environment. It was assumed that the insert was in contact with LN_2 on the bottom surface, whereas for the case where the pocket was machined in the insert, it was considered that all the walls of the machined pocket were in contact with LN_2 (Fig. 6). For the stress analysis the displacement of the bottom surface of the insert was fixed, and the load was applied at the tip of the tool. Both analyses were computed with implicit calculation. The main simulation parameters and the values assigned to the input parameters are presented in Table 3.

The magnitudes of the thermal and stress simulations were applied in a rectangular section which was calculated, assuming a depth of cut (a_p) of 1 mm and a tool-chip contact length of 0.25 mm. For orthogonal cutting of ASTM F-1537 CoCr alloys at cutting conditions of V_c = 60 m/min and f = 0.08 mm/rev, cutting force is around 330 N, as Baron et al. [44] stated. The tests carried out by these researchers in orthogonal cutting resulted in a specific cutting force (K_s) of roughly 4125 N/mm^2.

Taking the study of Baron et al as a reference, and assuming a security margin of 1.2, a specific cutting force of 5000 N/mm^2 was assumed for the simulation. Cutting parameters for the subsequent experimental tests were based on the investigation on cryogenic turning of Haynes 25 Cobalt based alloy by Sarikaya et al. [34]. Thus, as the feed and depth of cut values for the subsequent experimental plans were going to be f = 0.16 mm/rev and a_p = 1 mm, a load of 800 N applied at the tip of the insert was assumed for the stress simulation (as Expression 6 shows).

For the thermal simulation, a thermal load of 1100 K was taken, as it is a common temperature at the rake face of the tool when dry turning Cobalt based alloys.

$$Fc = a_p\, f\, K_s = 1\ \text{mm} \cdot 0.16\ {}^{\text{mm}}/_{\text{rev}} \cdot\ 5000\ {}^{\text{N}}/_{\text{mm}^2} = 800\ \text{N} \qquad (6)$$

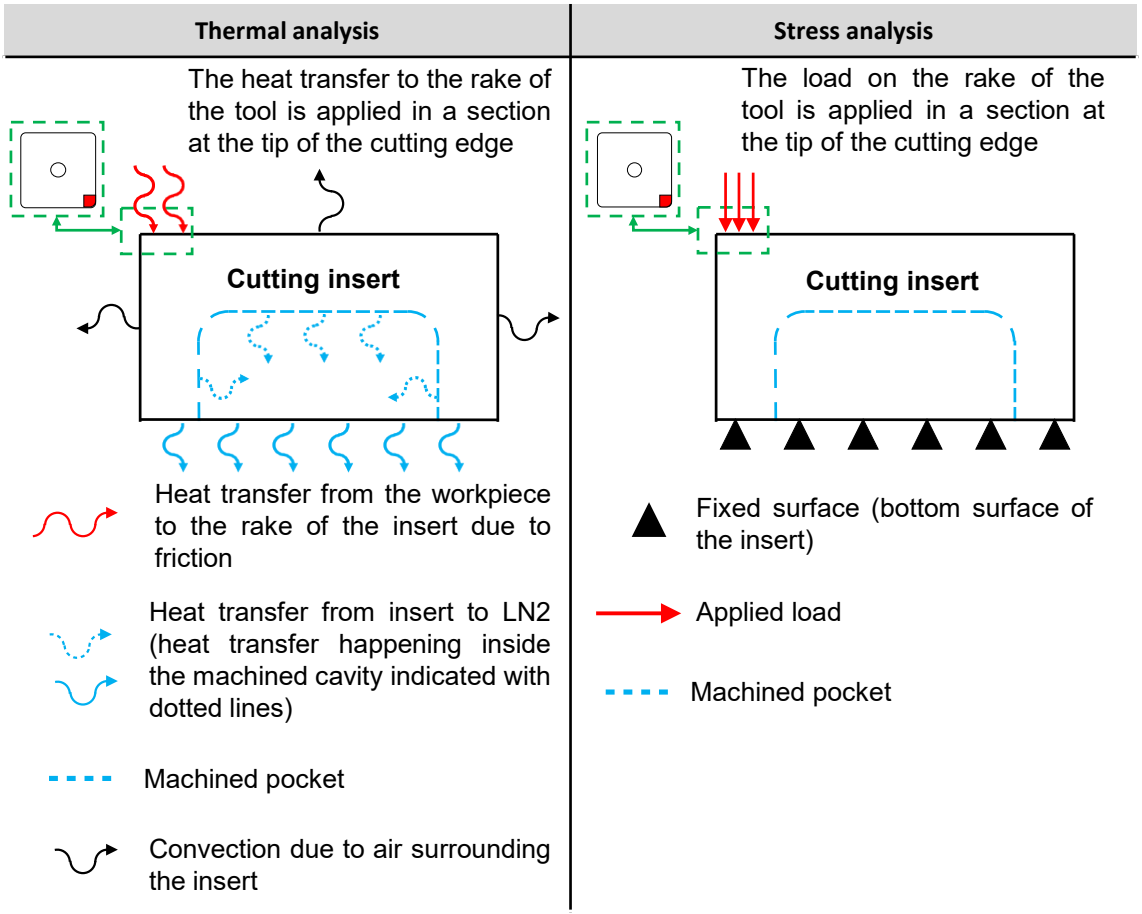

Fig. 6 Thermal and stress models used for FEM simulations

As the simulation results in Fig. 7 show, the Von Mises stress distribution on the insert is barely affected by the presence of the machined pocket. The side walls of the cavity were several times wider than the tool chip contact length, so that the material being cut was applying pressure on the whole thickness of the insert. Therefore, it can be stated that the modification of the insert has a negligible effect on the performance of the cutting tool, as the Von Mises stress distribution is similar to that of non-modified tools.

The contact area between chip and tool was calculated considering the cutting conditions for the subsequent experimental runs, nevertheless a side wall thickness of 1.5 mm will be greater than almost every uncut chip thickness and depth of cut employed in non-heavy machining. If cutting conditions were more severe a wider wall thickness and top wall thickness would be required, which would restrict the heat evacuation capacity of the tool. It can thus be concluded that the trade-off between deteriorated stress distribution and improved heat evacuation brought about by the machined pocket in the insert is optimal. Accordingly, the design of a cutting insert with a 9.7 mm^2 cavity and a 2 mm top wall thickness was validated.

Table 3: Simulation parameters for stiffness and thermal analysis of the modified insert

Simulation parameter	Stress analysis	Thermal analysis
Mesh details	Mesh size: 785 μm	Mesh size: 785 μm
	Element type: Hexahedral	Element type: Hexahedral
Load/thermal load details	Magnitude: 800 N	Magnitude: 1100 K
Boundary conditions	Fixed nodes in the bottom of the insert	LN_2 cold sink on bottom surface of the insert/cavity
Tool material properties	Yield strength of P10 grade carbide at 1100 K = 1780 MPa [41]	Thermal conductivity of P10 grade carbide at 1100 K = 64.4 W/m K [41]
	Young Modulus of P10 grade carbide at 1100 K = 320 GPa [41]	Specific heat capacity = 240 J/kg·K
	Poisson coefficient = 0.21	X
	Density = 8.7 kg/m^3 [2]	
LN_2 state	X	Convective coefficient of boiling saturated nitrogen at 313 K; h_{N2} = 0.25 W/m^2 K Convective coefficient of liquid nitrogen at 90 K; h_{LN2} = 250 W/m^2 K
Surrounding environment	X	Convective coefficient of still air at 298K; h_{AIR} = 15 W/m^2 K
Type of analysis	Static	Steady state

As for the thermal simulations, temperature gradients across the tool were expected such as those experienced by Minton et al. in their experimental trials with internally cooled diamond tools on turning Grade 2 CP Titanium [35]. Nevertheless, it can be clearly observed that the modification of the tool had significant effect on evacuating heat from the heat source, as a reduction of about 200 K in the body of the tool was achieved between modified and non-modified inserts.

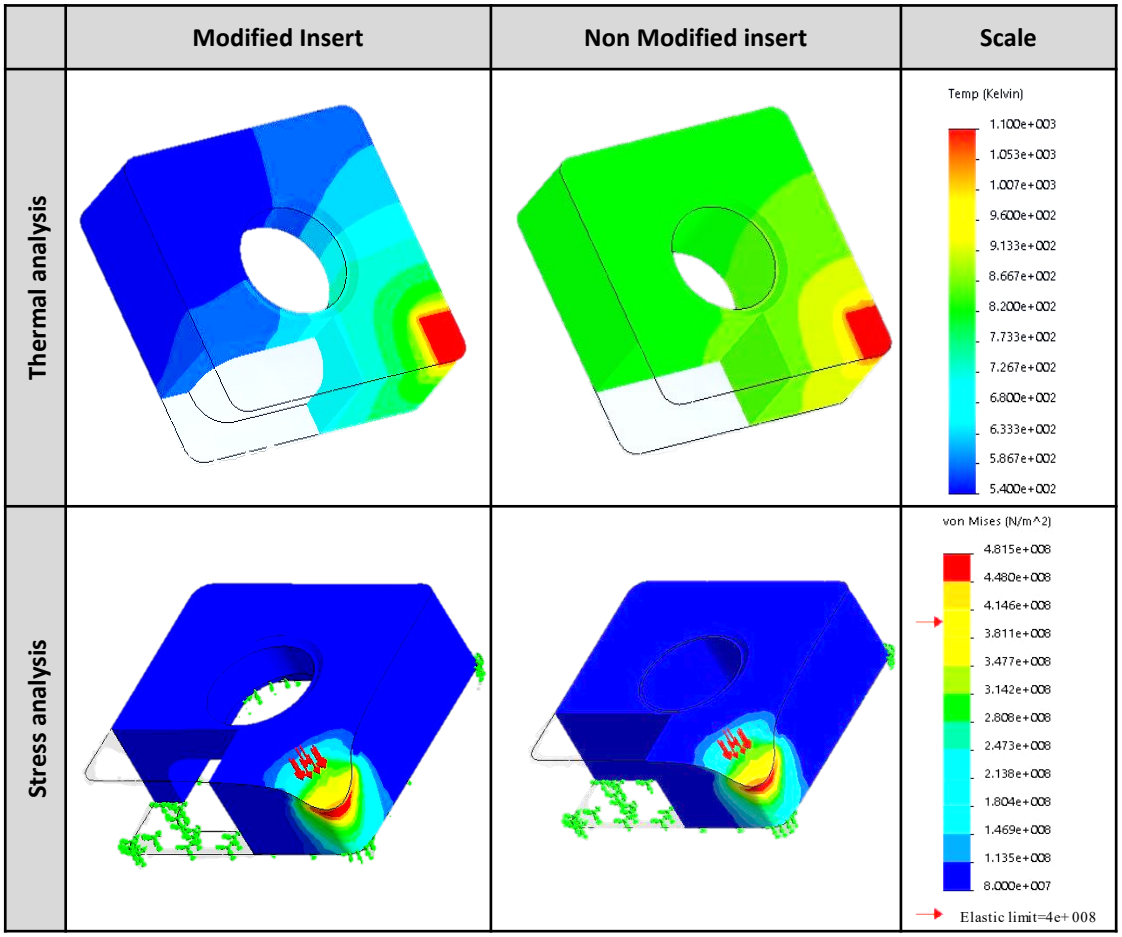

Fig. 7 Results of the stiffness and thermal analysis of the modified insert

2.3 Tool design

After validating the geometry of the designed cavity at the insert, modifications were performed on the tool holder and shim to allow LN_2 to circulate through the said cavity. As illustrated in Fig. 8, the LN_2 reaches the machined cavity through a channel machined in the back face of the shank of the tool, connected to the inlet which is machined in the shim of the tool. After exiting from an outlet also machined in the shim, the LN_2 is expelled from the upper face of the tool shank. Inlet and outlet channels were machined in the shim so as to enable rotation of the insert and make use of four cutting edges.

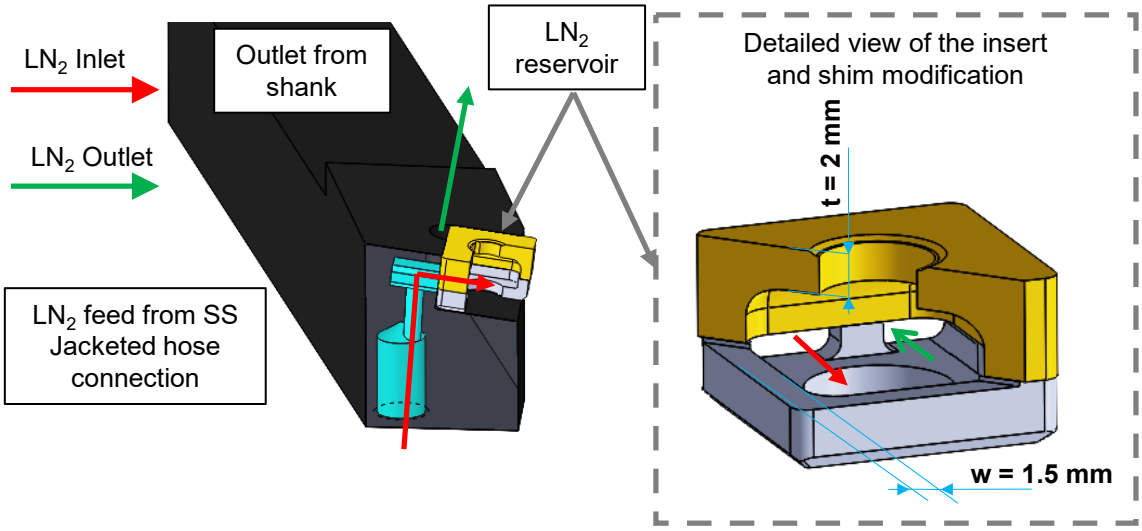

Fig. 8 Reservoir machined between the shim and the cutting insert, and the channel to allow the LN_2 to flow to the reservoir

The cutting tool was a coated carbide insert (T9100 SMNG120408-TS) with a nose radius of 0.8 mm. The cavity for LN_2 in the carbide insert was machined by sink Electro Discharge Machining (EDM), using a cobalt tungsten (CuW) electrode. The employed tool holder was a TungTurn DSBNR 2525M12 tool holder with -6° rake angle and 75° approach angle. The channels on the tool holder were machined by 5 axes milling and drilling, as shown in Fig. 9.

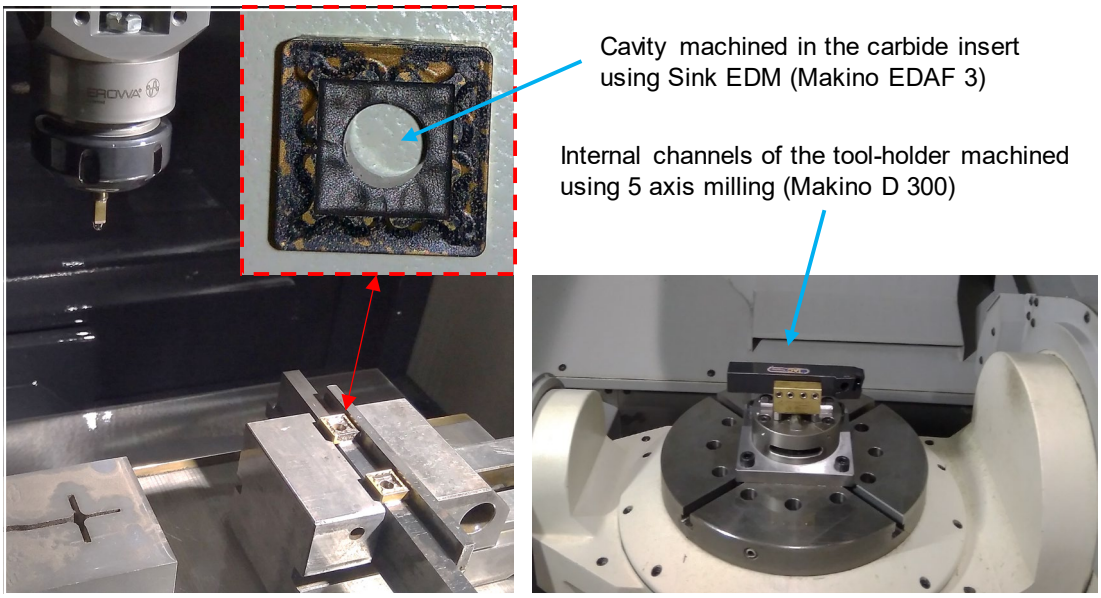

Fig. 9 Manufacturing process of the designed prototype

3 EXPERIMENTAL PROCEDURE

The main objective of this research is to analyse the feasibility of the proposed novel indirect cryogenic cooling system. For this purpose, a conventional indirect cryogenic cooling system and the newly proposed design were tested under dry and cryogenic conditions. Tests were carried out under dry conditions as it is important to assess the effect of employing an internally machined pocket on the stress distribution of the tool, and thus its potential damage. For this reason, four different cooling strategies were tested in the experiments, as shown in Table 4. Each testing condition was repeated 3 times to evaluate the repeatability of the machining operation.

When the modified inserts are employed the cavity or cooling reservoir created for the indirect cryogenic cooling is created by the cavities machined in both the insert and the shim of the cutting tool, as explained in the introduction in Fig. 1, c). On the other hand, for the non-modified inserts, the cavity is created just by the cavity machined at the shim and the bottom face of a conventional insert, like the Fig. 1, b) depicts, being this cavity smaller compared to when using modified inserts.

Table 4: Different cooling techniques tested for the prototype evaluation

Abreviation	Coolant	Type of insert used
A) Dry/Non-Mod	Dry	Non-modified insert (without pocket)
B) Dry/Mod	Dry	Modified insert (with machined pocket)
C) Cryo/Non-Mod	Cryogenic	Non-modified insert (without pocket)
D) Cryo/Mod	Cryogenic	Modified insert (with machined pocket)

3.1 Material properties

The workpiece material for the experimental tests was ASTM F-1537 CoCr alloy, the most relevant mechanical and thermal properties of which are summarized in Table 5.

Table 5: Most significant mechanical properties of biomedical CoCr ASTM F1537 [2] at room temperature.

Tensile strength, ultimate (MPa)	1403
Tensile strength, yield (MPa)	928
Elongation (%)	29
Young's Modulus (GPa)	283
Hardness (HRC)	40
Thermal Conductivity (W/(m K))	14.8
Specific heat capacity (J/(kg K))	452
Density (kg/m^3)	8250
Thermal diffusivity (m^2/s)	3.73E-06

3.2 Experimental set-up

The experiments were conducted on an OKUMA OSP-200LA CNC turning centre (rated output power of 15 kW). As Fig. 10 a) and b) show, the tool was mounted on a Kistler 9129 AA multi-component dynamometer employing a Kistler 9129 AE25 adaptor.

The LN_2 was supplied from the tank to the machined pocket through a stainless steel (SS) jacketed hose which was attached to the tool holder using a custom-made NPT 3/8 to M8 x 1.25 adapter (Fig. 10, d). LN_2 was delivered at a pressure of 1.5 bar from the low-pressure tank (tank pressure = 8 bar). As the dimension of the tested ASTM F-1537 CoCr alloy workpieces was small (Ø40 mm x 14 mm), a special threaded jig was fabricated to hold the workpieces

in the vice of the lathe Fig. 10, c). In this way the whole 14 mm of length of the workpiece could be machined, which was equivalent to 5 s of cutting time.

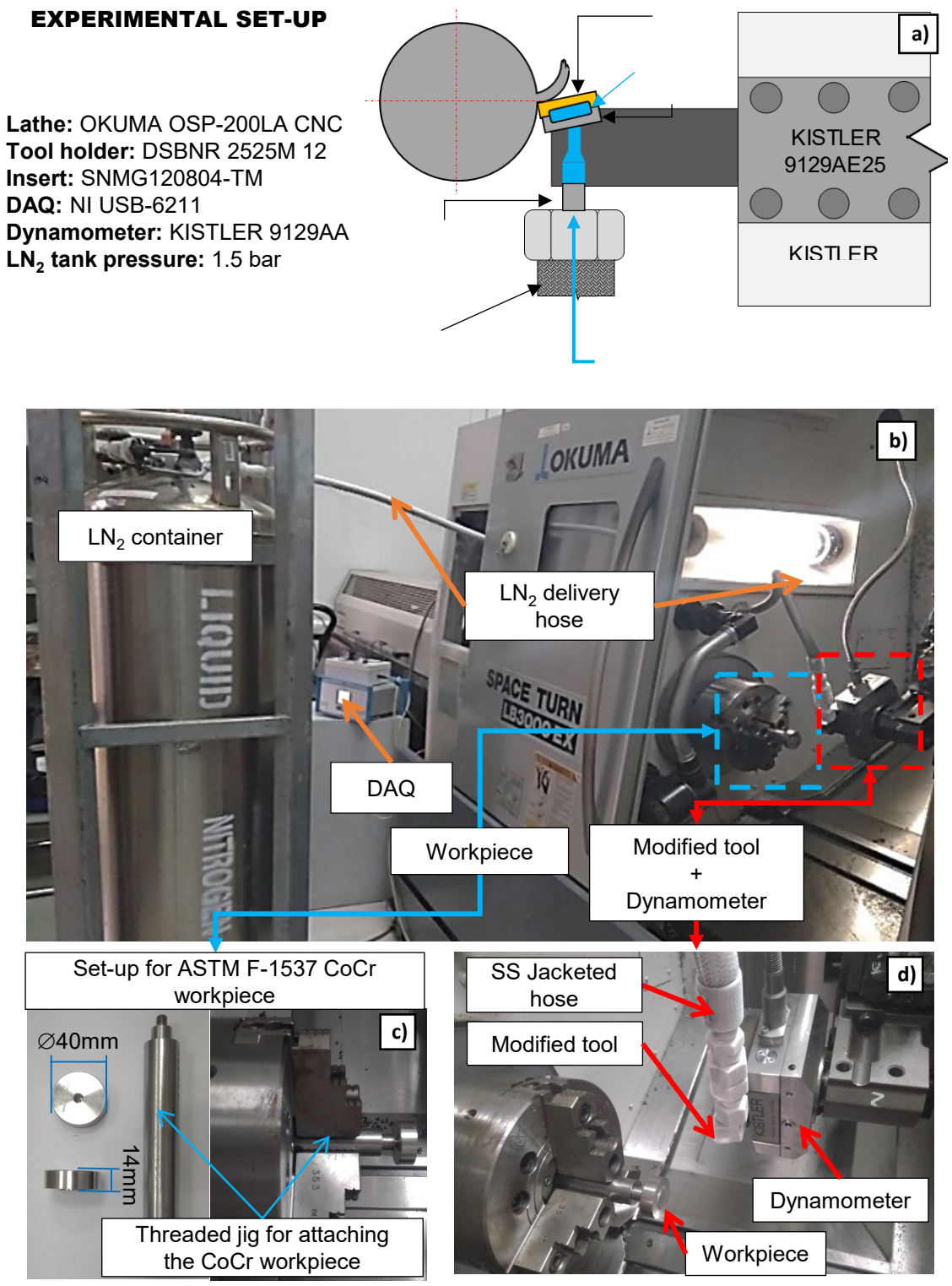

Fig. 10 Experimental set-up: a) Explanatory sketch of the experimental set-up, b) Cryogenic delivery system and Data Acquisition System (DAQ), c) Close-up view of the ASTM F-1537 CoCr workpiece set-up, d) Close-up view of the system mounted on the lathe

3.3 Cutting conditions and measurements

As specified in the experimental set-up description, a Kistler 9129AA dynamometer was mounted on the lathe turret to measure the cutting forces. The force signals were connected to a data acquisition system (DAQ) from National Instruments NI USB-6211, and subsequently amplified. The sampling frequency was 1 kHz and a Savitzky-Golay filter was employed to smooth the noise of the signal.

This filter fits consecutive sets of neighbouring data with, in this case, a third degree polynomial. The sample frame length to fit the polynomial and smooth the force signals correctly was 401 data points, as shown in Fig. 11. It is also worth mentioning that the noise in the signals from the feed force, F_f was, in most of the cases, higher than the other two cutting force components. It is believed that this noise is a consequence of the instability the threaded jig used to clamp the workpiece (shown in Fig. 10 c). The recorded signals in Fig. 11, show that all the 3 components of the cutting forces became stable in the last half of the duration of the cut. Therefore, it can be stated that the mean force values estimated from the acquired signals are reliable.

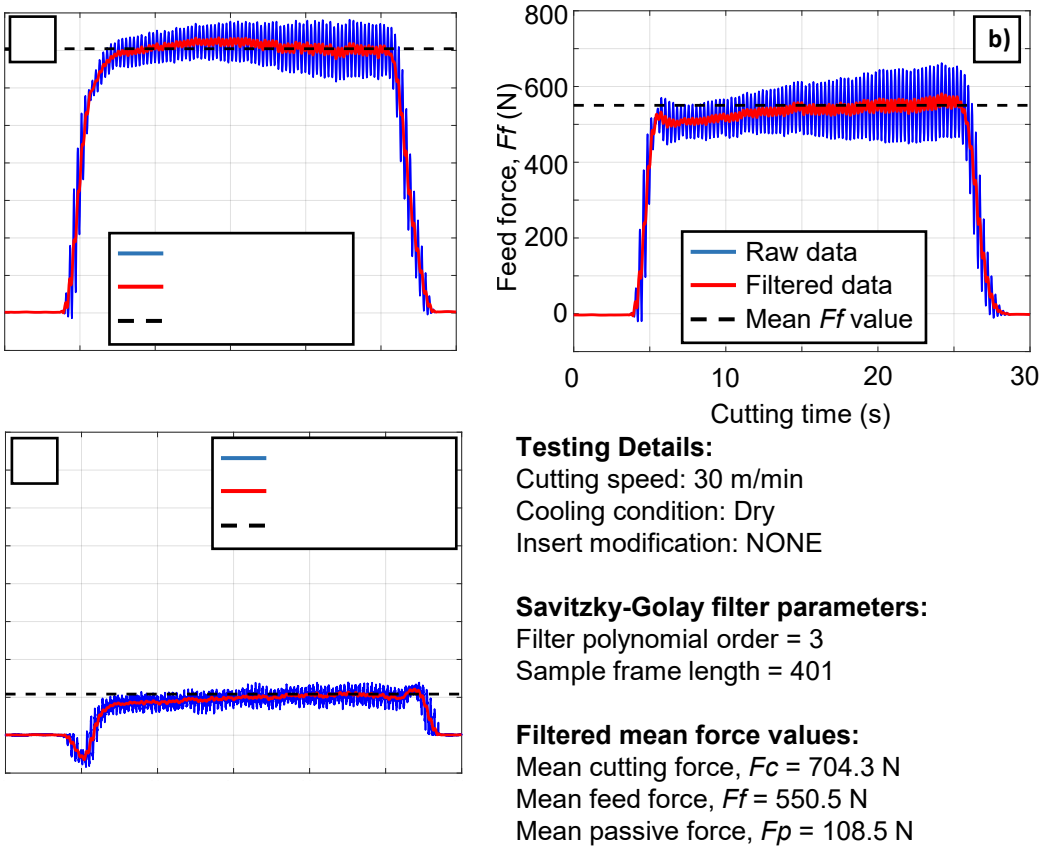

Fig. 11 Acquisition and smoothing of signals for the 3 force components using Savitzky-Golay filter: a) Cutting force, F_c; b) Feed force, F_f; c) Passive force, F_p

The machining tests were only carried out along 14 mm of cutting length. The duration of the cut varied for different tests as the diameter of the workpiece decreased and the spindle speed needed to be increased to maintain the cutting speed. Nevertheless, this length of cut was equivalent to 5 s of machining time for the shortest cut in duration, which was sufficient to stabilize the cutting forces. In addition, a fresh cutting edge was employed for each testing condition, so the tool wear was negligible after the machining test. Each testing condition was tested three times in

order to check the uncertainty. The cutting parameters used for each of the tested cooling conditions (explained in Table 4), are summarized in Table 6.

The specific cutting force obtained in dry conditions was 4375 N/mm2 ± 50 N (Fig. 11, b) Cutting force). This value is in agreement with the specific force measured by Baron et al. in orthogonal dry cutting of the ASTM F-1537 CoCr alloy [44]. The cutting force measured by these researchers in V_c = 60 m/min and f = 0.08 mm/rev cutting conditions was used as a reference value for the assumed cutting force in the FEM simulations of the present study.

Surface roughness was analysed employing a Bruker 3D optical profiler as shown in Fig. 12, a). The camera used in the profiler was a standard resolution colour camera with a 10x magnification lens (Fig. 12, b). A cut-off length of 250 μm was applied to the gaussian filter employed in the software eliminate the waviness of the cylindrical workpiece and measure the surface roughness correctly. Surface roughness was always measured while holding the workpiece with the threaded jig (Fig. 12 b), and the jig was always held in the same position in respect to the camera, so that measurements at the top surface of the cylindrical workpiece could be taken with repeatability. 5 profiles were measured in each of the analysed surfaces, then the average value was recorded for each of the trials.

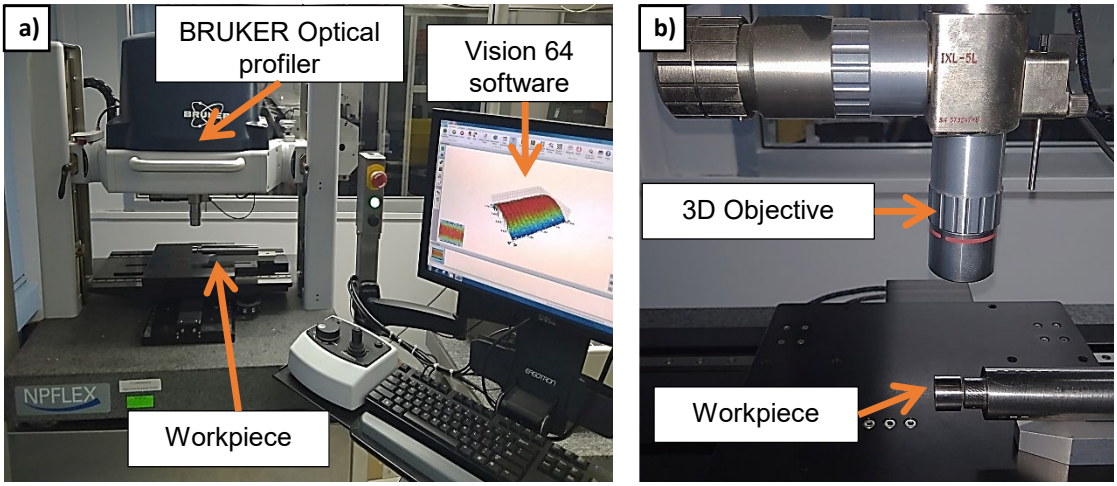

Fig. 12 a) Bruker optical profiler used for surface roughness analysis, b) Detailed view of the 10x resolution camera and the workpiece attached to the threaded jig

The machining tests were performed at different cutting speeds, while the feed and the depth of cut were fixed in order to evaluate the variation the output parameters at varying cutting speed. Cutting speeds varied from 30 m/min to 75 m/min at equal intervals, and the depth of cut was maintained constant at 1 mm. The feed and depth of cut values were maintained constant in all the experimental runs, at f = 0.16 mm/rev and a_p = 1 mm, respectively. These are the same feed and depth of cut values applied in the FEM simulations previously described.

Table 6: Cutting conditions employed in the experimental plan

Workpiece material	ASTM F-1537 CoCr alloy
Cutting speed(s), *Vc* (m/min)	30 – 45 – 60 – 75
Feed, *f* (mm/rev)	0.16
Depth of cut. a_p (mm)	1
Experimental output	Cutting forces and surface roughness

4 RESULTS AND DISCUSSION

4.1 Cutting force analysis

Three force components were recorded in the tests, using a multicomponent 9129AA Kistler dynamometer. Fig. 13 sets out the results obtained for these forces: F_p is the passive force (Fig. 13, a), F_c is the main cutting force (Fig. 13, b), and F_f corresponds to the feed force (Fig. 13, c). The values shown are an average of the three repetitions performed for each cutting speed and cooling condition. As can be seen in Fig. 13 b), the highest values of the cutting force were obtained for the main cutting force (F_c) when the cutting speed was the lowest.

Feed force (F_f) and the Cutting force (F_c) follow a downward trend as the cutting speed increases. Such a reduction in cutting force is attributed mainly to thermal softening of the workpiece and a slight decrease in the chip thickness at higher cutting speeds. Baron et al. [44] experienced the same results when the chip segment height decreased and cutting forces lowered with increasing cutting speed. This drop in cutting force (F_c) is more pronounced when machining the ASTM F-1537 CoCr workpiece in dry cutting conditions than under indirect cryogenic cooling. As can be seen in Fig. 13, when machining with the modified insert in dry conditions (“Dry/Mod”), the cutting force (F_c) decreases from 756 N to 640 N as the cutting speed increases from 30 m/min to 75 m/min. In the case of the modified insert under indirect cryogenic cooling (“Cryo/Mod”), the cutting force (F_c) drops from 615 N to 570 N.

A similar result was obtained by Dhananchezian et al. [50] when using indirect cryogenic cooling for turning another hard-to-cut material, Ti-6Al-4V. These authors noted that the effect of the indirect cryogenic cooling is greater at low cutting speeds since, at low material removal rates (MRR), a greater fraction of the heat stays in the tool while at higher MRR more heat is carried away by the chip.

Dhananchezian et al. [50] also attributed the decrease in cutting force brought about by the indirect cryogenic cooling to a reduction in adhesion in the chip-tool and tool-work interactions. In the study presented in this paper greater adhesion of workpiece material to the tool edge was observed when machining under dry conditions compared to indirect cryogenic cooling using the modified insert.

When employing indirect cryogenic cooling without the modified insert (“Cryo/Non-Mod”), a slight reduction in cutting forces could be observed when compared to dry cutting conditions, but this improvement was even smaller at high cutting speeds. It should also be noted that for the feed force component (Fig. 13, c) there was almost no difference in the recorded mean force values for dry machining (“Dry/Non-Mod “ and “Dry/Mod”) and cryogenic cooling without

the modified insert (“Cryo/Non.Mod”). The signals recorded of this force component (Fig. 11, c) had more noise than the cutting force and passive force signals (Fig. 11 a and b).

The cutting force values recorded in dry cutting show that the modification of the insert has little to no effect on them. As expected from the results of the FEM simulations shown in Fig. 7, the modification of the insert does not affect the robustness of the insert during short cuts, even at high cutting speeds. The effect of the machined pocket in tool life for longer duration cuts was not tested in the experimental runs, but it is expected that the modified insert would perform as a conventional insert, since the thickness of the side walls of the machined pocket are several times wider than the uncut chip thickness when machining hard-to-cut materials.

Passive cutting forces (F_p) were noticeably lower and showed less change when varying cutting or cooling conditions than the other two force components, as seen in Fig. 13, a).

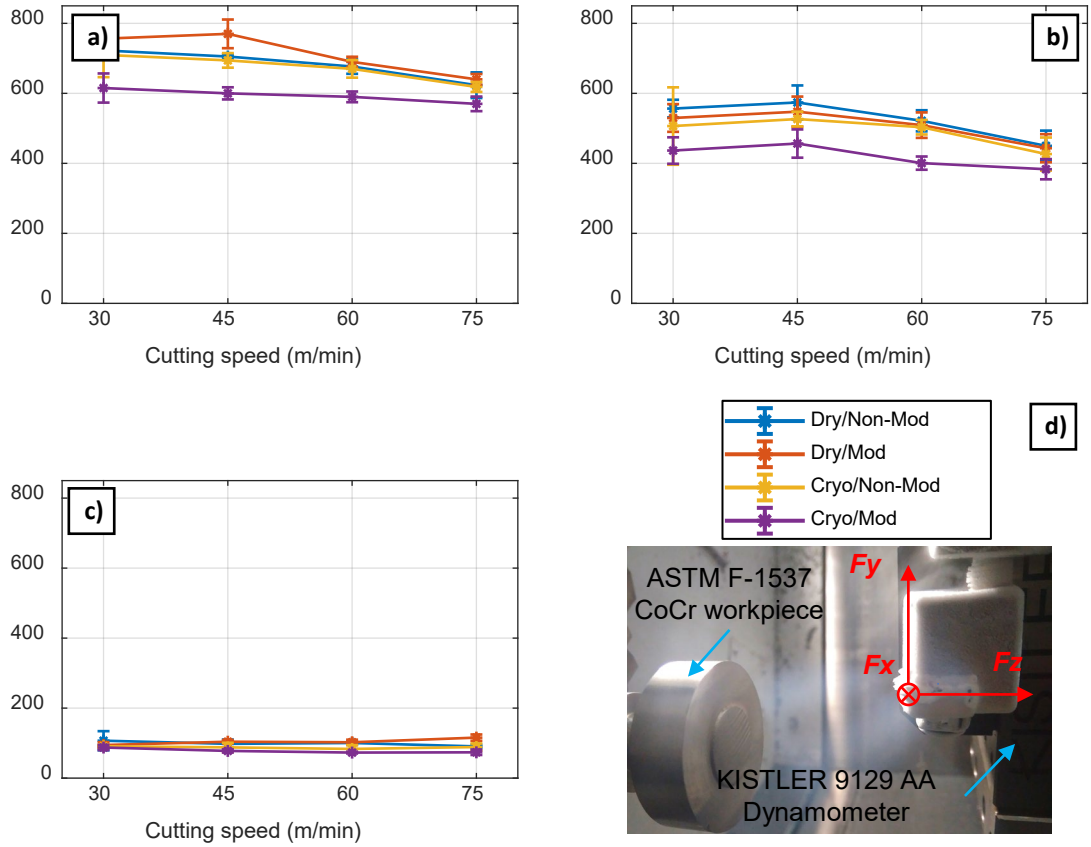

Fig. 13 Variation of 3 force components when machining the ASTM F-1537 CoCr alloy with cutting speed for dry and cryogenic cooling, with modified and non-modified inserts.
a) cutting force, b) feed force and c) passive force. d) Close-up view of the internal cryogenically cooled tool mounted on the dynamometer

The lowest cutting force values were obtained with the modified cutting insert under indirect cryogenic cooling conditions (“Cryo/Mod”). On the other hand, using indirect cryogenic cooling with the non-modified insert (“Cryo/Non-Mod”) achieved similar cutting force values to when machining in dry conditions, at high cutting speeds. This phenomenon can be attributed to a greater amount of LN_2 stored under the rake face when using modified inserts compared to conventional cutting inserts, which helped to maintain the strength and hardness of tool material [50]. It also highlights that the effectiveness of indirect cryogenic cooling systems is highly dependent upon the amount of

surface available for heat exchange and thickness of the insert, as previous studies have also pointed out [17], [31]. It is important to note that using the modified tool under cryogenic cooling conditions (“Cryo/Mod”), brings about a 12% reduction in the cutting force, compared to state-of-the-art indirect cryogenic cooling systems (“Cryo/Non-Mod”), where the cavity is created just using the shim.

4.2 Surface roughness analysis

All measurements were taken at the top surface of the cylindrical workpiece and in the middle of its length. Fig. 14 sets out the average surface roughness values Ra obtained with all four cooling conditions under different cutting speeds. The figure shows that the best surface finish results were obtained when employing the novel prototype presented in this study under indirect cryogenic cooling conditions (“Cryo/Mod”).

It should be noted that indirect cryogenic cooling of the tool produced better results in comparison to dry cutting at low cutting speeds (“Cryo/Non-Mod” and “Cryo/Mod” over “Dry/Non-Mod” and “Dry/Mod”). As the cutting speed was increased past 45 m/min, the surface roughness started to deteriorate, and the indirect cryogenic cooling was no longer beneficial for dry machining with non-modified tools. In Fig. 14 it can be seen that the surface roughness values obtained with “Cryo/Non-Mod” are similar to the ones obtained with “Dry/Non-Mod” and “Dry/Mod”.

This deterioration of surface roughness for cutting speeds higher than 45 m/min was also observed by Sarikaya and Güllü when machining the cobalt-based alloy Haynes 25 [51]. As they stated, the optimal window for machining such alloys is between 15 m/min and 45 m/min. A similar process window was proposed by Yingfei et al. [46] when milling the cobalt-based alloy Stellite 6, as they obtained the best surface finish results when milling in dry conditions between 25 m/min and 40 m/min.

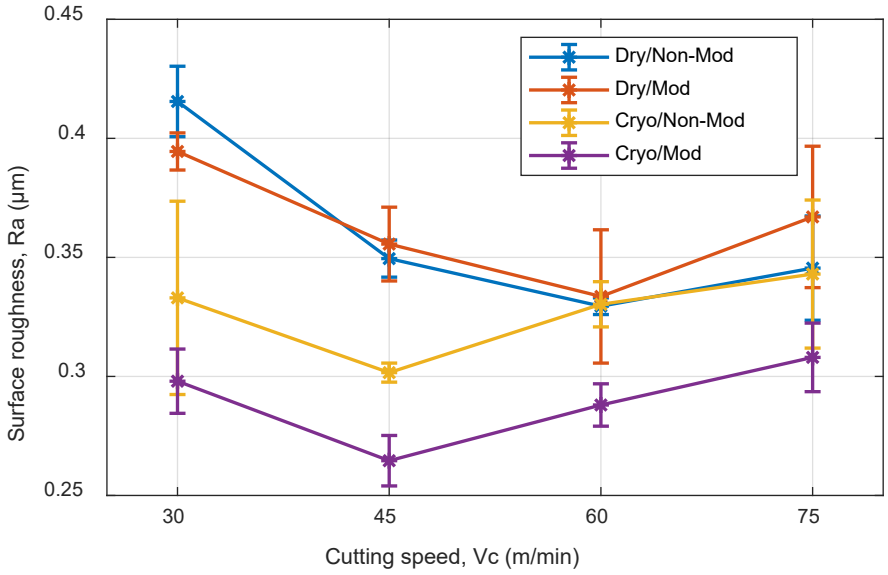

Fig. 14 Variation of surface roughness (Ra) when machining the ASTM F-1537 CoCr alloy with cutting speed for dry and cryogenic cooling, with modified and non-modified inserts.

At low cutting speed values, the cooling effect of the indirect cryogenic cooling system is more noticeable than at high cutting speed values. This can be also observed in the cutting force results, as the reduction in cutting forces brought up by the indirect cryogenic cooling is greater at low cutting speeds compared to high cutting speeds. At

cutting speeds above 60 m/min the cutting force and surface roughness values yielded by the indirect cryogenic cooling system without the modified insert (“Cryo/Non-mod”) are similar to the ones obtained in dry cutting conditions.

When employing indirect cryogenic cooling, the modified tool (“Cryo/Mod”) obtained better surface roughness results than the non-modified tool (“Cryo/Non-Mod”). The improvement in surface finish was 12% for cutting speeds between 45 m/min and 60 m/min**.** This improvement may be related to improved cooling of the tool when employing the novel modified system proposed in this study. As Shao et al. stated, at high cutting loads (Vc = 45 m/min and f = 0.25 mm/rev), adhesion problems appeared when turning a Stellite 12 cobalt-based alloy, which caused a poor surface finish [52]. Better cooling of the tool can prevent adhesion problems, which can ensure a better surface finish.

The improvement in surface roughness resulting from indirect cryogenic cooling with the modified insert (“Cryo/Mod”) is even more pronounced when compared to dry machining conditions (“Dry/Non-Mod” and “Dry/Mod”). Using the modified insert with indirect cryogenic cooling improved the surface roughness by 25% for cutting speeds between 30 m/min and 45 m/min. It also resulted in an improvement of 12% against dry machining for higher cutting speeds (60 m/min and 75 m/min).

4.3 Economic analysis of the prototype

In this study a novel prototype which employs LN_2 for indirectly cooling the cutting zone is presented. As discussed in the experimental results, this prototype shows reduction in cutting forces and an improved surface finish in comparison to dry cutting and state-of-the-art indirect cryogenic cooling solutions. Nevertheless, there are other aspects to be considered in order to select this cooling approach instead of other cooling/lubrication methods available in the industry.

When employing dry machining the use of the cutting fluid is completely eliminated. This reduces the heat evacuation from the cutting zone, and therefore an adequate selection of the tool material and process parameters is required [53], in order to reduce tool wear and improve surface integrity of the machined part. In dry cutting there is no water or atmosphere contamination, and as no oils are employed there is no need to clean the machined parts, or the chips for recycling. Nevertheless, the tool life is reduced, and in applications like hole making, chip evacuation becomes complicated [15].

In conventional flood cooling cutting fluids are oil or water-based mixtures and their function is to cool and lubricate. The use of conventional cutting fluids also helps reduce the power consumption of the machine and protect the machined surface from corrosion, improve chip evacuations, as well as increase tool life by slowing down tool wear mechanisms. This allows to increase cutting speed which in turn increases productivity [54]. Nevertheless, there are several environmental legislations regarding disposal costs and workers and environmental safety which make the use of these fluids more costly than other more environmentally sustainable alternatives [15]. It has been proven that conventional cutting fluids create several health hazards for workers apart from contaminating the water, soil and the atmosphere [9], and the cost of disposal and posterior cleaning of the machined part achieves around 16-18 % of the total cost of production [15]. The cleaning cost becomes even more critical for industries like prosthetics since the contamination of the machined part with oils can create allergic reactions on the patient [11].

MQL uses a mix of compressed air with a reduced amount of oil in form of droplets which allows to reduce the fluid consumption while still lubricating the cutting zone, but no cooling is provided [55]. The initial cost of the equipment is lower than for flood cooling since no fluid disposal or recirculation systems are required, as the cutting fluid is

provided in very small quantities [56]. However, as oils are used in the cutting process the machined parts and the chips are still contaminated, so it is required to clean them. In addition, as MQL is projected to the cutting zone in the form of aerosol, a cloud of oil mist is formed in the working area, and this poses a health hazard to operators, therefore mist extractors would be required to eliminate the oil particles from the air [57].

Sub-zero cooling uses liquified gases like LN_2 or liquid carbon dioxide (LCO_2) in order to cool down the cutting zone during machining. LCO_2 is stored in pressurized tanks at room temperature, and when released to atmospheric pressure, the sudden drop in pressure makes the fluid change phase to a solid/gas mixture with a temperature of around -78 ºC. On the other hand LN_2 is stored in liquid state at -197 ºC at room temperature, therefore, insulated tanks and hoses are required for its storage, which increases the cost of the equipment compared to LCO_2 [58].

Several studies have been carried out showing that sub-zero coolants improve tool life and surface integrity when machining hard-to-cut alloys [31]–[33], nevertheless, there are some cases in which the sub-zero cooling assisted machining obtained worse results than conventional flood cooling or dry machining [26], [27]. Even if their feasibility is still not certain researchers keep studying different techniques to apply sub-zero coolants to machining because they are environmentally friendly. Using these liquefied gases as coolants creates no hazard for the atmosphere or the worker as the gases being released are already present in the atmosphere.

The main problem of these cooling solutions is the initial cost of the equipment [59]. However, the cost of the cooling fluid is competitive against the conventional cutting fluids due to a lower flow, no cost of fluid treatment after machining and no cleaning of the machined parts or produced chips [15].

Table 7 presents a qualitative estimation of economic and environmental impact of various lubrication/cooling systems used in machining operations, taking into account the above considerations. After this table, it is considered that liquefied gases could be as well a clear alternative to other proposed solutions at present, if proper working conditions (tool holder, insert, gas flow rate and pressure, area of application) are found.

Table 7: Qualitative economic and environmental analysis of the designed prototype

	DRY	**Flood cooling**	**MQL**	**LCO_2 cooling**	**Indirect LN_2 cooling**
Cost of the cooling fluid	*	**	**	***	***
Equipment costs	*	****	***	****	*****
Fluid consumption	*	*****	**	*	***
Tool cost	*****	*	*	**	***
Cleaning cost	*	*****	****	*	*
Disposal cost	*	*****	****	*	*

In the specific application of indirect cryogenic cooling that is presented in this study only LN_2 can be used as coolant. This is because LCO_2 needs to be released to atmospheric pressure in order to experience a drop in temperature, and in an indirect cooling system the cooling liquid is not released near the cutting zone. For this reason the equipment costs are higher for indirect LN_2 cooling in comparison to LCO_2 cooling, as shown in Table 7.

For the prototype presented in this research study, the cutting inserts were modified using sink EDM and the tool holder using a 5 axis CNC machine, therefore the tooling cost is higher compared to the tools employed in any other cooling technique showed in Table 7. However, if the modified inserts were produced as standards ones using powder metallurgy, their cost would decrease, as the production time of each insert would be reduced substantially. Similarly, would happen for the tool holder. Also, the indirect cryogenic cooling system with the modified insert helped to reduce cutting forces and improve surface roughness in comparison to dry cutting, mainly at low cutting speeds, the authors believe that this prototype should be used in roughing or semi-finishing operations. As discussed in the introduction the reduction of cutting forces helps to reduce dimensional errors when turning hard-to-cut materials [4] and a proper surface finish in the semi-finishing operations reduces the machining time of finishing operations, which are more complex and costly [6].

5 CONCLUSIONS

A novel indirect cryogenic cooling system was presented in this study for machining the hard-to-cut ASTM F-1537 CoCr alloy. Turning experiments were conducted under different cutting speeds and cooling conditions to test the feasibility of this new prototype for manufacturing processes which need to eliminate oil-based lubricants (e.g., the machining of medical grade materials). This new design differs from state-of-the-art indirect cryogenic cooling systems in that it has a pocket machined in the cutting insert employing sink EDM. The principal findings are summarized as follows:

- The present study has showed the feasibility of modifying conventional cutting inserts in order to enhance the cooling capability of indirect cryogenic cooling techniques without altering the stress distribution of the tool, reducing cutting forces and improving the roughness of the machined surface. Further tests analysing the influence of these modifications in tool life are required.
- The new design proposed in this study increases the available heat exchange surface and reduces the insert thickness. This allows the LN_2 to flow nearer to the rake face and enhances heat evacuation capability without excessively compromising the tool damage, as the FEM simulations show.
- When employing indirect cryogenic cooling, the new modified tool (“Cryo/Mod”) reduced the cutting force (F_y) by 12% in comparison with state-of-the-art indirect cryogenic cooling designs (“Cryo/Non-Mod”), and by 15 % in comparison with dry cutting (“Dry/Non-Mod” and “Dry/Mod”). It is believed that this improvement is due to the reduction of plastic deformation of the material during cutting, as the tool was cooled while the workpiece remained ductile. Similar conclusions were drawn by Dhananchezian et al. [50] when comparing indirect cryogenic cooling to conventional emulsion lubrication for turning the hard-to-cut Ti - 6Al - 4V alloy.
- Surface roughness was improved by 12% when utilizing the modified insert instead of a non-modified insert under indirect cryogenic conditions (“Cryo/Mod” over “Cryo/Non-Mod”). These results may be due to a reduction in adhesion problems brought about by the increased cooling capacity of the modified cutting tool.
- Surface roughness results show that the improvement resulting from indirect cooling systems is limited, and affected by the severity of the cutting conditions. When employing indirect cryogenic cooling with a small cavity for the cryogenic media (“Cryo/Non-Mod”) the surface roughness values were improved by 20% at low

cutting speeds when compared to dry machining (“Dry/Non-Mod” and “Dry/Mod”), but no improvement was observed at cutting speeds above 60 m/min. On the other hand, when employing a greater cavity for the cryogenic media (“Cryo/Mod”), surface roughness improved by 25% at low cutting speeds (between 30 m/min and 45 m/min), and a lower improvement of 12% was measured at higher cutting speeds (60 m/min and 75 m/min). This highlights the importance of available surface for heat exchange in order to enhance tool cooling and improve surface finish of the machined surface.

- Making a trade-off between cutting force and surface roughness, it would seem that for the selected feed per revolution (0.16 mm/rev) a suitable cutting speed could be in the range of 45-60 m/min. More in-depth studies need to be carried out to confirm this assumption.
- Due to the prototype having a greater heat evacuation capacity at low cutting speeds, and being the modification of the cutting inserts by EDM process relatively cheap, the authors suggest that the presented indirect cryogenic cooling system should be used for roughing or semi-finishing operations. Having lower cutting forces may increase tool life and improve dimensional accuracy or roughed parts. This along with an improved surface finish can reduce the cost of subsequent finishing operations.
- The qualitative estimation of economic and environmental impact of various lubrication/cooling systems used in machining operations show that the use of liquefied gases could be as well an alternative to other proposed solutions at present, if proper working conditions (tool holder, insert, gas flow rate and pressure, area of application) are found.

6 ACKNOWLEDGEMENTS

The authors of this report would like to express their very great appreciation to Mr. Dylan Khor from Tungaloy Cutting Tool (Thailand) Co., Ltd. for providing the all the cutting tools necessary for the project; to Haimer Asia Pacific Ltd. for providing the tool holder required to perform the modifications, and in like manner to Mr. Cha-Hliang Goonjam, Application Manager from Makino (Thailand) Co. Ltd. for carrying out the manufacturing operations in the cutting tools which were essential for this project. The authors would also like to thank the Basque Government for the support provided by the PROCODA project (Code KK-2019/00004).

7 REFERENCES

[1] A. Shokrani, V. Dhokia, and S. T. Newman, “Cryogenic High Speed Machining of Cobalt Chromium Alloy,” *Procedia CIRP*, vol. 46, pp. 404–407, 2016.

[2] D. D. T. C. Material, S. Baron, E. Ahearne, P. Connolly, S. Keaveney, and G. Byrne, “An Assessment of Medical Grade Cobalt Chromium Alloy ASTM F1537 as a ‘ Difficult-to-Cut (DTC)’ Material,” in *Proceedings of MTTRF*, 2015, no. January 2016.

[3] M. Sarıkaya and A. Güllü, “Examining of Tool Wear in Cryogenic Machining of Cobalt-Based Haynes 25 Superalloy,” *Int. J. Mater. Metall. Eng.*, vol. 9, no. 8, pp. 984–988, 2015.

[4] M. Sarıkaya, V. Yılmaz, and A. Güllü, “Analysis of cutting parameters and cooling/lubrication methods for sustainable machining in turning of Haynes 25 superalloy,” *J. Clean. Prod.*, vol. 133, pp. 172–181, 2016.

[5] Y.-H. Kim, A. Ritchie, and C. Hardaker, “Surface Roughness of Ceramic Femoral Heads After in Vivo Transfer of Metal : Correlation to Polyethylene Wear,” *J. og Bone Jt. Surg.*, 2005.

[6] C. Courbon, D. Kramar, P. Krajnik, F. Pusavec, J. Rech, and J. Kopac, “Investigation of machining

performance in high-pressure jet assisted turning of Inconel 718: An experimental study," *Int. J. Mach. Tools Manuf.*, vol. 49, no. 14, pp. 1114–1125, 2009.

[7] E. Brinksmeier, D. Meyer, A. G. Huesmann-Cordes, and C. Herrmann, "Metalworking fluids - Mechanisms and performance," *CIRP Ann. - Manuf. Technol.*, vol. 64, no. 2, pp. 605–628, 2015.

[8] K. Busch, C. Hochmuth, B. Pause, A. Stoll, and R. Wertheim, "Investigation of Cooling and Lubrication Strategies for Machining High-temperature Alloys," *Procedia CIRP*, vol. 41, pp. 835–840, 2016.

[9] F. Pusavec, P. Krajnik, and J. Kopac, "Transitioning to sustainable production - Part I: application on machining technologies," *J. Clean. Prod.*, vol. 18, no. 2, pp. 174–184, 2010.

[10] S. Spiegelberg, K. Deluzio, and O. Muratoglu, "Extractable residue from recalled Inter-OPTM acetabular shells," in *49th Annual Meeting of the Orthopaedic Research Society*, 2003, vol. 28, p. 1346.

[11] L. A. Bonsignore, V. M. Goldberg, and E. M. Greenfield, "Machine Oil Inhibits the Osseointegration of Orthopaedic Implants by Impairing Osteoblast Attachment and Spreading," *Orthop. Res. Soc.*, no. July, pp. 979–987, 2015.

[12] K. Saptaji, M. A. Gebremariam, and M. A. B. M. Azhari, "Machining of biocompatible materials: a review," *Int. J. Adv. Manuf. Technol.*, vol. 97, no. 5, pp. 2255–2292, 2018.

[13] P. Campbell, J. Mirra, and I. Catelas, "Hispatology of tissues from Inter-OP Acetabular sockets," in *48th Annual Meeting of the Orthopaedic Research Society*, 2000, p. 187.

[14] R. W. Maruda, G. M. Krolczyk, S. Wojciechowski, K. Zak, W. Habrat, and P. Nieslony, "Effects of extreme pressure and anti-wear additives on surface topography and tool wear during MQCL turning of AISI 1045 steel," *J. Mech. Sci. Technol.*, vol. 32, no. 4, pp. 1585–1591, 2018.

[15] E. Benedicto, D. Carou, and E. M. Rubio, "Technical, Economic and Environmental Review of the Lubrication/Cooling Systems Used in Machining Processes," *Procedia Eng.*, vol. 184, pp. 99–116, 2017.

[16] B. Sen, M. Mia, G. M. Krolczyk, U. K. Mandal, and S. P. Mondal, *Eco-Friendly Cutting Fluids in Minimum Quantity Lubrication Assisted Machining: A Review on the Perception of Sustainable Manufacturing*, no. 0123456789. Korean Society for Precision Engineering, 2019.

[17] S. Y. Hong, Y. Ding, and W. cheol Jeong, "Friction and cutting forces in cryogenic machining of Ti-6Al-4V," *Int. J. Mach. Tools Manuf.*, vol. 41, no. 15, pp. 2271–2285, 2001.

[18] F. Pusavec *et al.*, "Sustainable machining of high temperature Nickel alloy - Inconel 718: Part 1 - Predictive performance models," *J. Clean. Prod.*, vol. 81, pp. 255–269, 2014.

[19] M. Hardt, F. Klocke, B. Döbbeler, M. Binder, and I. S. Jawahir, "Experimental study on surface integrity of cryogenically machined Ti-6Al-4V alloy for biomedical devices," *Procedia CIRP*, vol. 71, pp. 181–186, 2018.

[20] Y. Kaynak, "Evaluation of machining performance in cryogenic machining of Inconel 718 and comparison with dry and MQL machining," *Int. J. Adv. Manuf. Technol.*, vol. 72, no. 5–8, pp. 919–933, 2014.

[21] Y. Ayed, G. Germain, A. P. Melsio, P. Kowalewski, and D. Locufier, “Impact of supply conditions of liquid nitrogen on tool wear and surface integrity when machining the Ti-6Al-4V titanium alloy,” *Int. J. Adv. Manuf. Technol.*, vol. 93, no. 1–4, pp. 1199–1206, 2017.

[22] M. Mia *et al.*, “Multi-objective optimization and life cycle assessment of eco-friendly cryogenic N2 assisted turning of Ti-6Al-4V,” *J. Clean. Prod.*, vol. 210, pp. 121–133, 2019.

[23] M. Hribersek, V. Sajn, F. Pusavec, J. Rech, and J. Kopac, “The Procedure of Solving the Inverse Problem for Determining Surface Heat Transfer Coefficient between Liquefied Nitrogen and Inconel 718 Workpiece in Cryogenic Machining,” *Procedia CIRP*, vol. 58, no. May, pp. 617–622, 2017.

[24] P. Lequien, “Etude fondamentale de l ’ assistance cryogénique pour application au fraisage du Ti6Al4V,” 2018.

[25] T. Heep, C. Bickert, and E. Abele, “Application of Carbon Dioxide Snow in Machining of CGI using an Additively Manufactured Turning Tool,” *J. Manuf. Mater. Process.*, vol. 3, no. 1, p. 15, 2019.

[26] A. Iturbe, E. Hormaetxe, A. Garay, and P. J. Arrazola, “Surface Integrity Analysis when Machining Inconel 718 with Conventional and Cryogenic Cooling,” *Procedia CIRP*, vol. 45, no. Table 1, pp. 67–70, 2016.

[27] S. Isakson, M. I. Sadik, A. Malakizadi, and P. Krajnik, “Effect of cryogenic cooling and tool wear on surface integrity of turned Ti-6Al-4V,” *Procedia CIRP*, vol. 71, pp. 254–259, 2018.

[28] S. Y. Hong, I. Markus, and W. Jeong, “New cooling approach and tool life improvement in cryogenic machining of titanium alloy Ti-6Al-4V,” *Int. J. Mach. Tools Manuf.*, vol. 41, no. 8, pp. 2256–2260, 2001.

[29] S. Y. Hong and Y. Ding, “Cooling approaches and cutting temperatures in cryogenic machining of Ti-6Al-4V,” *Int. J. Mach. Tools Manuf.*, vol. 41, no. 10, pp. 1417–1437, Aug. 2001.

[30] Y. Yildiz and M. Nalbant, “A review of cryogenic cooling in machining processes,” *Int. J. Mach. Tools Manuf.*, vol. 48, no. 9, pp. 947–964, 2008.

[31] Z. Y. Wang and K. P. Rajurkar, “Cryogenic machining of hard-to-cut materials,” *Wear*, vol. 239, no. 2, pp. 168–175, 2000.

[32] M. I. Ahmed, A. F. Ismail, Y. A. Abakr, and A. K. M. N. Amin, “Effectiveness of cryogenic machining with modified tool holder,” *J. Mater. Process. Technol.*, vol. 185, no. 1–3, pp. 91–96, 2007.

[33] A. A. Khan and M. I. Ahmed, “Improving tool life using cryogenic cooling,” *J. Mater. Process. Technol.*, vol. 196, no. 1–3, pp. 149–154, 2008.

[34] M. Sarikaya and A. Güllü, “Examining of Tool Wear in Cryogenic Machining of,” *Int. J. Mater. Metall. Eng.*, vol. 9, no. 8, pp. 751–755, 2015.

[35] T. Minton, S. Ghani, F. Sammler, R. Bateman, P. Fürstmann, and M. Roeder, “International Journal of Machine Tools & Manufacture Temperature of internally-cooled diamond-coated tools for dry-cutting titanium,” *Int. J. Mach. Tools Manuf.*, vol. 75, pp. 27–35, 2013.

[36] J. C. Rozzi and J. K. Sanders, “The Experimental and Theoretical Evaluation of an Indirect Cooling System for Machining,” *J. Heat Transfer*, vol. 133, no. March 2011, pp. 1–10, 2016.

[37] B. Haddag, S. Atlati, M. Nouari, and M. Zenasni, “Analysis of the heat transfer at the tool–workpiece interface in machining: determination of heat generation and heat transfer coefficients,” *Heat Mass Transf.*, vol. 51, Jan. 2015.

[38] R. Komanduri and Z. B. Hou, “Thermal modeling of the metal cutting process - Part III: Temperature rise distribution due to the combined effects of shear plane heat source and the tool-chip interface frictional heat source,” *Int. J. Mech. Sci.*, vol. 43, no. 1, pp. 89–107, 2001.

[39] T. Kitagawa, A. Kubo, and K. Maekawa, “Temperature and wear of cutting tools in high-speed machining of Inconel 718 and Ti-6Al-6V-2Sn,” *Wear*, vol. 202, no. 2, pp. 142–148, 1997.

[40] Haynes International, “HAYNES ® 25 alloy Principle Features,” 2015.

[41] A. Nordgrena, B. Z. Samanib, and R. M. Saoubic, “Experimental Study and Modelling of Plastic Deformation of Cemented Carbide Tools in Turning,” *Procedia CIRP*, vol. 14, pp. 599–604, 2014.

[42] A. Aherwar, S. Gwalior, A. Singh, and A. Patnaik, “Study on mechanical and wear characterization of novel Co30Cr4Mo biomedical alloy with added nickel under dry and wet sliding conditions using Taguchi approach,” *Proc. Inst. Mech. Eng. Part L J. Mater. Des. Appl.*, no. April, 2016.

[43] K. J. Bhansali, “ADHESIVE WEAR OF NICKEL- AND COBALT-BASE ALLOYS,” in *International Conference on Wear of Materials*, 1980, vol. 60, no. April 1979, pp. 95–110.

[44] S. Baron and E. Ahearne, “An investigation of force components in orthogonal cutting of medical grade cobalt–chromium alloy (ASTM F1537),” *Proc. Inst. Mech. Eng. Part H J. Eng. Med.*, vol. 231, p. 095441191769018, Feb. 2017.

[45] S. Baron and E. Ahearne, “An investigation of force components in orthogonal cutting of medical grade cobalt chromium alloy (ASTM F1537),” no. July, 2018.

[46] G. Yingfei, P. M. de Escalona, and A. Galloway, “Influence of Cutting Parameters and Tool Wear on the Surface Integrity of Cobalt-Based Stellite 6 Alloy When Machined Under a Dry Cutting Environment,” *J. Mater. Eng. Perform.*, vol. 26, no. 1, pp. 312–326, 2017.

[47] Y. A. Çengel and A. J. Ghajar, *Heat and Mass Transfer*, 5th ed. Mc Graw Hill, 1395.

[48] J. E. Jensen, W. A. Tuttle, R. B. Stewart, H. Brechna, and A. G. Prodell, “Properties of Nitrogen,” *Brookhaven Natl. Lab. Sel. Cryog. Data Noteb.*, 1980.

[49] J. M. Tarragó, S. Dorvlo, I. Al-Dawery, and L. Llanes, “Strength degradation of cemented carbides due to thermal shock,” 2015.

[50] M. Dhananchezian, D. Satishkumar, S. Palani, and N. Ramprakash, “Study the Effect of Cryogenic Cooling With Modified Cutting Tool Insert in the Turning of Ti-6al-4v Alloy,” *Int. J. Eng. Res. Technol.*, vol. 2, pp. 2541–2547, Sep. 2013.

[51] M. Sarıkaya and A. Güllü, “The Analysis of Process Parameters for Turning Cobalt-Based Super Alloy Haynes 25 / L 605 Using Design of Experiment,” *Solid State Phenom.*, vol. 220–221, pp. 749–753, Jan. 2015.

[52] H. Shao, L. Li, L. J. Liu, and S. Z. Zhang, “Study on machinability of a stellite alloy with uncoated and coated carbide tools in turning,” *J. Manuf. Process.*, vol. 15, pp. 673–681, Oct. 2013.

[53] A. Hosseini Tazehkandi, F. Pilehvarian, and B. Davoodi, “Experimental investigation on removing cutting fluid from turning of Inconel 725 with coated carbide tools,” *J. Clean. Prod.*, vol. 80, pp. 271–281, 2014.

[54] M. Soković and K. Mijanović, “Ecological aspects of the cutting fluids and its influence on quantifiable parameters of the cutting processes,” *J. Mater. Process. Technol.*, vol. 109, no. 1–2, pp. 181–189, 2001.

[55] D. Dudzinski, A. Devillez, A. Moufki, D. Larrouquère, V. Zerrouki, and J. Vigneau, “A review of developments towards dry and high speed machining of Inconel 718 alloy,” *Int. J. Mach. Tools Manuf.*, vol. 44, no. 4, pp. 439–456, 2004.

[56] A. D. Jayal, A. K. Balaji, R. Sesek, A. Gaul, and D. R. Lillquist, “Machining performance and health effects of cutting fluid application in drilling of A390.0 cast aluminum alloy,” *J. Manuf. Process.*, vol. 9, no. 2, pp. 137–146, 2007.

[57] E. O. Ezugwu, “Key improvements in the machining of difficult-to-cut aerospace superalloys,” *Int. J. Mach. Tools Manuf.*, vol. 45, no. 12–13, pp. 1353–1367, 2005.

[58] P. Blau, K. Busch, M. Dix, C. Hochmuth, A. Stoll, and R. Wertheim, “Flushing strategies for high performance, efficient and environmentally friendly cutting,” *Procedia CIRP*, vol. 26, pp. 361–366, 2015.

[59] F. Pusavec, D. Kramar, P. Krajnik, and J. Kopac, “Transitioning to sustainable production - Part II: Evaluation of sustainable machining technologies,” *J. Clean. Prod.*, vol. 18, no. 12, pp. 1211–1221, 2010.